RSC Advances

PAPER

View Article Online
View Journal | View Issue

Cite this: *RSC Adv.*, 2021, **11**, 20687

Room temperature facile synthesis of olivine-Co_2SiO_4 nanoparticles utilizing a mechanochemical method

Phuong Q. H. Nguyen,[a] Dongzhou Zhang,[ab] Robert Rapp,[a] John P. Bradley[a] and Przemyslaw Dera*[a]

Received 8th April 2021
Accepted 27th May 2021

DOI: 10.1039/d1ra02760c

rsc.li/rsc-advances

Co_2SiO_4 is a ceramic pigment and promising battery material of significant technological interest, as well as a model end-member of one of the most important mineral families in the Earth's crust and upper mantle. All previously developed methods for synthesis of Co_2SiO_4 require high-temperature processing, which promotes grain growth, while the nanocrystalline form is required for some important technological applications. Here, we report a successful method for synthesizing nanocrystalline Co_2SiO_4 *via* a simple and inexpensive high-energy ball milling mechanochemical process. Products of the synthesis were characterized by a combination of XRD and TEM, and their crystal structures and elemental compositions are reported.

Silicates with M_2SiO_4 formula and olivine-structure, where M is mainly Mg and Fe, and containing small amounts of Mn, Ni, Co and Ca, are of fundamental importance in geology and mineralogy, as they are predominant minerals in the crust and upper mantle of the Earth. The olivine structure is one of the most robust crystallographic arrangements, able to accommodate not only a variety of metal cations, but also other types of anionic groups. Naturally occurring silicates recognized as minerals include simple binary compounds: forsterite (Mg_2SiO_4), fayalite (Fe_2SiO_4), tephroite (Mn_2SiO_4), liebenbergite (Ni_2SiO_4), and larnite (Ca_2SiO_4), as well as Ca-containing ternary silicates: monticellite ($CaMgSiO_4$), kirschsteinite ($CaFeSiO_4$) and glaucochroite ($CaMnSiO_4$). In addition to silicates, germanate GeO_4^{2-}, SiS_4^{2-}, and GeS_4^{2-} as well as phosphate PO_4^{3-} compounds can crystallize in the olivine structure.

The Fe- and Mg- end-members of the naturally occurring $(Fe_{1-x}Mg_x)_2SiO_4$ solid solution have been the subject of intensive studies in mineralogy, as refractories, lithium battery materials, and for carbon sequestration.[1–3] Mg_2SiO_4 occurs in three well-known equilibrium polymorphs, referred to as α (forsterite, orthorhombic *Pnma* olivine structure), β (wadsleyite, orthorhombic *Imma* spinelloid structure), and γ (ringwoodite, cubic spinel structure) phases. The latter two of these polymorphs (β and γ) are stable at elevated pressure and temperature conditions, yet both can be metastably quenched. One of the less-studied olivine-type silicates, Co_2SiO_4, also exists in three structural forms, analogous to Mg_2SiO_4 phases. Ringwood *et al.* determined that the transformation to the ringwoodite form of the Co_2SiO_4 takes place at 7 GPa and 700 °C and Morimoto *et al.* synthesized, analysed, and compared the crystal structures of all three Co_2SiO_4 polymorphs.[4,5]

Olivine-type Co_2SiO_4 has been synthesized by a variety of traditional methods, including precipitation, hydrothermal, and sol–gel, all of which involve multi-step synthesis and/or heating to above 500 °C,[6–8] resulting in crystal growth and particle aggregation. For example, Co_2SiO_4 can be produced by heating a mixture of Co_3O_4 and SiO_2 at 1350 °C.[4] Yatabe *et al.* synthesized Co_2SiO_4 by sintering an amorphous precipitate, formed by mixing sodium metasilicate and cobalt nitrate solutions, at 1200 °C.[8] Taguchi *et al.* synthesized Co_2SiO_4 by hydrothermal reaction of $CoCl_2 \cdot 6H_2O$ and $Na_2SiO_3 \cdot 9H_2O$, and subsequent calcination of the resulting precursor at 950 °C.[7] Guo *et al.* also synthesized Co-olivine nanoparticles by solid-state reaction of cobalt acetate and tetraethyl orthosilicate followed by calcination at 500–700 °C.[9] Stoia *et al.* used a sol–gel method and tetraethylorthosilicate, cobalt nitrate and organic diols to synthesize Co_2SiO_4/SiO_2 nanocomposite after calcination at 700 °C.[6] Finally, Bayat *et al.* recently reported synthesis of Co_2SiO_4 nanostructures and nanocomposites *via* the sol–gel method using cobalt(II) acetate tetrahydrate, tetraethyl orthosilicate, NH_3 and carbohydrate at calcination temperatures of 500–700 °C.[10]

The nanoparticulate Co_2SiO_4 was shown to exhibit improved optical and electrochemical performance.[9,10] The conventional ceramic synthetic processes, which result in grain sizes exceeding 1 micrometer, cannot produce the grain shapes and morphologies required for some of technological applications.

[a]*Hawaii Institute of Geophysics and Planetology, University of Hawai'i at Manoa, 1680 East-West Road, Honolulu, HI 96822, USA. E-mail: pdera@hawaii.edu; Fax: +1-808-956-3188; Tel: +1-808-956-6347*

[b]*GeoSoilEnviro CARS, Argonne National Laboratory, University of Chicago, Argonne, IL 60439, USA*

Mechanochemical activation by high-energy milling has become a widely used method for solid state synthesis, representing an alternative to high temperature processes.[11] The recent report of successful mechanochemical synthesis of Fe_2SiO_4 raises the strong probability that other olivine compounds might be obtained using a similar approach.[12] To this end, we have investigated the one-step synthesis of a stoichiometric mixture of CoO and SiO_2 at ambient temperature. To the best of our knowledge, this approach for synthesizing olivine-structured Co_2SiO_4 has not been tried before.

Using a high-energy Retsch MM400 oscillating mill, mixtures of CoO and SiO_2 (2 : 1 molar ratio) were loaded in 25 mL tungsten carbide (WC) jars, and mechanically milled dry with two 15 mm diameter WC balls (40 : 1 ball to powder ratio) at oscillating frequency of 30 Hz, for various times, ranging from 5 to 180 minutes. Because the linear motion component in the grinding jars of oscillating mills is more pronounced, compressive stress is enhanced at the expense of the shear component, when compared to the more common planetary mills. An optional annealing stage involving heating of the milled product at 500, 750, or 1000 °C for 12 hours, was also carried out for the 180 minute-milled sample. Milling experiments performed in air or under controlled atmosphere (Ar) showed no difference in processing outcomes. Macroscopic temperature monitoring of the milling jar using an attached thermocouple indicated that a maximum temperature of 75 °C was reached during milling trials. The issue of thermal evolution during ball milling has been a subject of many previous studies, and the term "ambient temperature process" is quite widely accepted in the mechanochemical literature. For example, Schmidt *et al.* discusses the temperature progression in a mixer ball mill, while Takacs and McHenry *et al.* talks about shaker and planetary mills. Our temperature monitoring results are consistent with these earlier studies.[15,16] The phase composition of the starting materials, milled products, and annealed samples were tested using Bruker D8 Advance high-resolution powder diffraction with 3 kW CuKα source and LynxEye XE detector in Bragg-Brentano parafocusing geometry.

Fig. 1 shows a comparison of the powder XRD patterns of the starting mixture and samples milled for different duration. The cobalt oxide starting material was found to contain 13% of spinel-type Co_3O_4. Short milling times (less than 45 minutes) only produce changes in the average grain size of the sample and lattice strain, which as indicated by increasing diffraction peak width, but no new peaks are observed. Milling for 60 minutes results in the appearance of the characteristic pattern for orthorhombic olivine. Complete conversion of starting materials to Co_2SiO_4 was observed after 75 minutes. The width of the diffraction peaks of the product phase was similar to the width of the peaks for the precursors after milling for 45 minutes, indicative of sub-micrometer grain size. Milling for 720 minutes does not produce any further changes in the Co-olivine product, but results in increased contamination of the sample with WC debris from the grinding elements.

The milling process in an oscillating mill is believed to proceed at only slightly elevated average temperatures (below 100 °C), though individual ball-and-sample impacts may involve

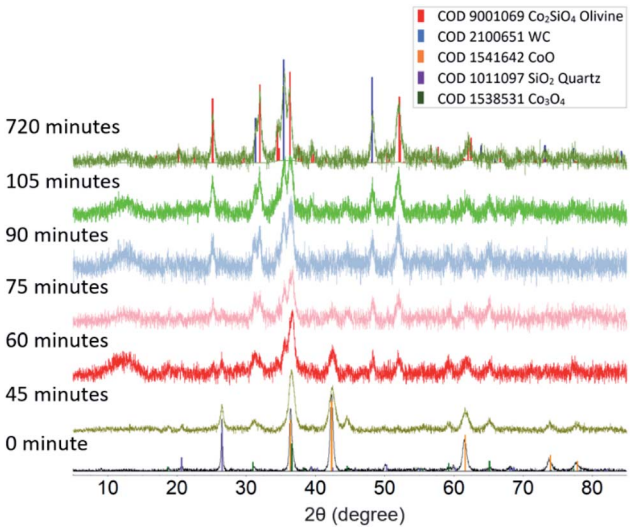

Fig. 1 Powder XRD patterns of 2 : 1 molar ratio CoO and SiO_2 mixture after various milling times.

significant localized heating. Therefore, our solid-state milling-induced synthesis of Co_2SiO_4 is essentially a room temperature reaction. In order to test the effect of annealing on the mechanochemically-synthesized Co-olivine, a series of heating experiments, at 500, 750 and 1000 °C for 12 h was conducted. Results of powder XRD analysis of the annealed samples are shown in Fig. 2. Heating at 500 °C produces only minor changes in the grain size (grain growth) and anneals some of the residual strain, as evidenced by the changes in the peak widths. A marked change in the peak width of the olivine phase (significant grain growth) was observed after heating above 750 °C. Further heating to 1000 °C induced a reaction of the WC debris with the olivine sample, resulted in the formation of approximately 15% $CoWO_4$.

Fig. 3 illustrates the results of Rietveld refinements of the 180- minute-milled sample both with and without annealing,

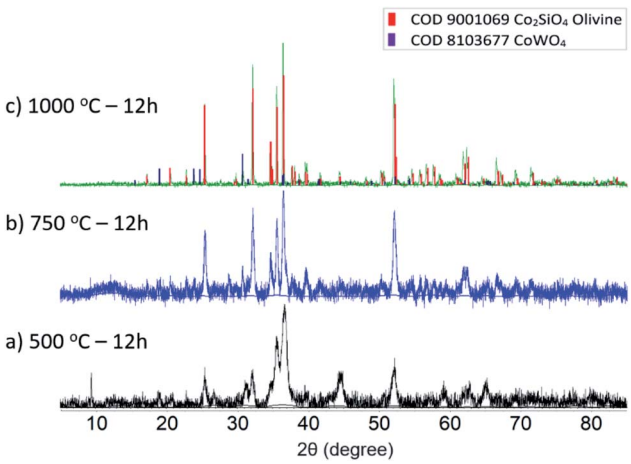

Fig. 2 Powder XRD spectra of ball milled 2 : 1 molar ratio CoO and SiO_2 mixture after annealing for 12 hours at (a) 500 °C (b) 750 °C (c) 1000 °C.

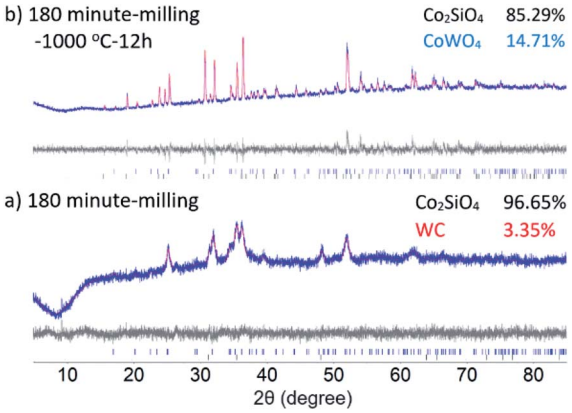

Fig. 3 Rietveld refinement of the (a) 2 : 1 molar ratio of CoO and SiO_2 after (a) 180 minutes milling time (b) 180 minute-milled mixture followed by heating at 1000 °C for 12 hours. The bottom curve shows the difference between the observed and calculated intensities. Tick marks below indicate peak positions for cobalt silicate and WC/$CoWO_4$.

which converge to a final-figure-of-merit $R_{wp} = 3.128$ and 1.886, respectively. Rietveld analysis was conducted using Bruker TOPAS 5.[13] The starting models for the Co_2SiO_4, WC, $CoWO_4$ structures were taken from PDF 00-015-0865, PDF 00-051-0939, and PDF 00-015-0867, respectively.[14] Refinement included optimization of background, phase fractions, unit cell parameters, peak profiles (controlled by grain size and strain models), site occupancies for non-oxygen atoms, and atomic displacement parameters. Fractional atomic coordinates were kept fixed at the literature values. Refined unit cell parameters are in excellent agreement with literature data,[5] and refined site occupancy factors for Si and Co sites were very close to 1.0 (Table 1). Quantitative analysis of grain size using the Hall-Williamson method implemented in TOPAS 5 and refined peak profiles indicated an increase in average grain size from 96 nm in the 180 minute-milled sample to 250 nm after heat treatment.

In order to determine the elemental composition and assess chemical homogeneity of the milled product, we used an 80–300 keV high-base Titan (FEI Thermo-Fisher) scanning transmission electron microscope equipped with a solid state Si(Li) energy-dispersive X-ray detector (Genesis 4000, EDAX). Bright-field and darkfield images were acquired in scanning transmission ("STEM") mode and the crystal structures of grains were assessed using selected area electron diffraction (SAED). Compositions were measured by energy-dispersive X-ray spectroscopy ("EDS") and quantified using a Cliff-Lorimer thin-film approximation and correction factors ("K factors") derived from thin film standards. Representative STEM micrographs of the mechanochemically-synthesized Co_2SiO_4 after 180 minutes of milling time at different magnifications are displayed in Fig. 4a–d. The product consists of particles that show fairly broad size distribution, with many smaller grains aggregated together in large clumps. Attempt to break out these clumps ultrasonically produced little significant change in the end product. A representative SAED pattern of the milled sample (Fig. 4e) shows high degrees of spottiness in the diffraction rings, consistent with the nanocrystalline nature of the as-synthesized Co_2SiO_4. Indexing of the SAED pattern revealed the presence of (112), (120), and (131) single crystal peaks of Co_2SiO_4. Particle size analysis performed with the TEM images (Fig. 4f) indicates an average particle size of 157 nm with a broad range in size distribution (28 to 651 nm diameter).

An EDS spectrum obtained with the TEM instrument on the Co_2SiO_4 sample milled for 180 minutes (Fig. 5) depicts the sole presence of Co, Si, and O elements. Quantitative analysis of elemental mass percentages based on this spectrum suggests

Table 1 Unit cell parameters obtained from Rietveld refinement of the synthesized Co_2SiO_4 before and after heating. SOF is site occupancy factor[a]

	105 min	180 min	Heat 750 °C	Heat 1000 °C
a (Å)	4.79(9)	4.79(6)	4.785(14)	4.7855(9)
b (Å)	10.34(19)	10.31(13)	10.30(3)	10.311(2)
c (Å)	5.98(11)	6.01(8)	6.006(17)	6.0105(12)
V (Å^3)	296.2(10)	296.8(8)	295.8(6)	296.38(12)
SOF [Co_1]	1.01(4)	1.02(3)	1.003(19)	0.964(13)
SOF [Co_2]	1.02(4)	0.99(3)	0.995(16)	0.955(11)
SOF [Si]	1.00(6)	1.00(7)	0.991(5)	0.992(4)
Si–O bond (Å)	1.614(22)	1.613(22)	1.612(21)	1.613(12)
Co–O bond (Å)	2.145(71)	2.143(69)	2.142(68)	2.141(69)
Rietveld (R_{wp})	2.203	1.886	2.458	3.128

[a] Standard deviations in parentheses are in unit of the last digit stated.

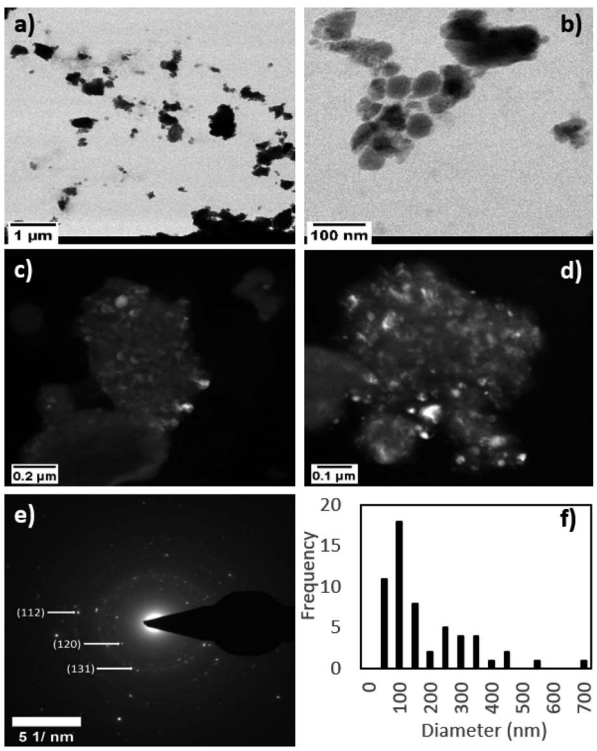

Fig. 4 Brightfield (a) and (b), and darkfield (c), and (d) STEM images at different magnifications (e) selected area electron diffraction (SAED) data and (f) grain size distribution of 180 minute-milled Co_2SiO_4.

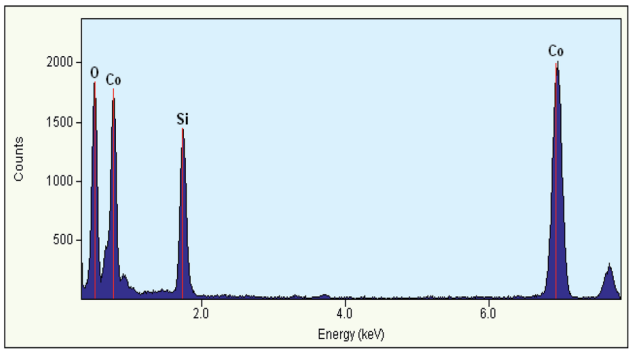

Fig. 5 Representative STEM-EDS spectrum of 180 minute-milled Co_2SiO_4.

Table 2 Quantitative elemental analysis Co_2SiO_4 obtained after 180 minutes of milling, from STEM-EDS spectrum

Element	Weight%	Atomic%	Uncert.%
O (K)	27.74	53.44	0.38
Si (K)	15.26	16.75	0.19
Co (K)	56.98	29.79	0.42

an empirical formula of Co_2SiO_4 (Table 2). WC debris, despite being detected by powder XRD (Fig. 1), was not present in the EDS spectrum. This observation further confirms our suspicion that the milling product is a mixture of olivine Co_2SiO_4 and contaminant WC.

We conducted a series of comparative experiments with grinding jars and balls made of stainless steel. In all of these experiments, we noted (based on XRF results and Rietveld refinements) that the product olivine phase incorporates some amount of iron into its crystal structure. The details of these experiments will be discussed in a separate publication.

In summary, this communication presents a straightforward means of synthesizing nanocrystalline Co_2SiO_4 directly from oxide precursors. No traces of the high-pressure forms of Co_2SiO_4 were detected in any of the synthesis experiments, suggesting that the peak impact conditions were not high enough to promote polymorphic transformation. This synthesis has been shown to proceed at ambient temperature, and without contingent inert atmospheric control. Although WC debris is present in the final milled sample, the nature of the product raises the plausibility that WC can be removed by the development of a proper solid–solid separation technique. Annealing of the milled product at high temperatures results in a solid-state substitution reaction between the as-synthesized olivine Co_2SiO_4 and WC, leading to the formation $CoWO_4$ species. Given the nanocrystalline nature of the product and simple reaction activation by milling, it is recommended that the as-synthesized Co_2SiO_4 merits further study in material development applications.

Conflicts of interest

There are no conflicts to declare.

Acknowledgements

We acknowledge the financial support of this work provided by the Office of Naval Research, Department of Navy's Historically Black Colleges and Universities/Minority Institutions, the Materials for Thermal and Chemical Extreme program, grant number FOA N00014-19-S-F004. RR has been supported by NSF EAR grant 1829273.

Notes and references

1 V. Goldschmidt, *Ind. Eng. Chem.*, 1938, **30**(1), 32–34.
2 M. Leonardi, M. Villacampa and J. C. Menéndez, *Chem. Sci.*, 2018, **9**(8), 2042–2064.
3 Q. R. Miller, H. T. Schaef, J. P. Kaszuba, G. Gadikota, B. P. McGrail and K. M. Rosso, *Environ. Sci. Technol. Lett.*, 2019, **6**(8), 431–442.
4 A. Ringwood, *Nature*, 1963, **198**(4875), 79–80.
5 N. Morimoto, M. Tokonami, M. Watanabe and K. Koto, *Am. Mineral.*, 1974, **59**(5–6), 475–485.
6 M. Stoia, M. Stefanescu, T. Dippong, O. Stefanescu and P. Barvinschi, *J. Sol-Gel Sci. Technol.*, 2010, **54**(1), 49–56.
7 H. Taguchi, Y. Takeda and H. Shibahara, *Mater. Lett.*, 2002, **52**(6), 412–416.
8 J. Yatabe, T. Sugizaki, T. Ikawa and T. Kageyama, *J. Ceram. Soc. Jpn.*, 1997, **105**(1218), 188–191.
9 P. Guo and C. Wang, *RSC Adv.*, 2015, **5**(86), 70661–70667.
10 S. Bayat, A. Sobhani and M. Salavati-Niasari, *J. Mater. Sci.: Mater. Electron.*, 2018, **29**(9), 7077–7089.
11 Q. Zhang, S. Ge, H. Xue, X. Wang, H. Sun and A. Li, *RSC Adv.*, 2014, **4**(102), 58260–58264.
12 V. Šepelák, M. Myndyk, M. Fabián, K. L. Da Silva, A. Feldhoff, D. Menzel, M. Ghafari, H. Hahn, P. Heitjans and K. D. Becker, *Chem. Commun.*, 2012, **48**(90), 11121–11123.
13 A. A. Coelho, *J. Appl. Crystallogr.*, 2018, **51**(1), 210–218.
14 S. Gates-Rector and T. Blanton, *Powder Diffr.*, 2019, **34**(4), 352–360.
15 R. Schmidt, H. M. Scholze and A. Stolle, *Int. J. Ind. Chem.*, 2016, **7**, 181.
16 L. Takacs and J. S. McHenry, *J. Mater. Sci.*, 2006, **41**, 5246.